Cancer Research

Podoplanin-Positive Fibroblasts Enhance Lung Adenocarcinoma Tumor Formation: Podoplanin in Fibroblast Functions for Tumor Progression

Ayuko Hoshino[1,2], Genichiro Ishii[2], Takashi Ito[1,2], Kazuhiko Aoyagi[4], Yoichi Ohtaki[3], Kanji Nagai[3], Hiroki Sasaki[4], and Atsushi Ochiai[1,2]

Abstract

During the metastatic process, cancer cells interact with vascular adventitial fibroblasts (VAF), which are the main components of the outermost connective tissue layer of blood vessels. This activity suggests the presence of a specific tumor microenvironment in the perivascular area. The s.c. coinjection of human lung adenocarcinoma cell lines (A549, PC-14, and CRL-5807) and human VAF (hVAF) resulted in a high rate of tumor formation, compared with the coinjection of these cell lines and human lung tissue-derived fibroblasts (hLF). A cDNA microarray analysis revealed a higher expression level of podoplanin in hVAFs than in hLFs (4.7-fold). Flow cytometry analysis also showed a higher expression level of podoplanin in hVAFs (43% $\pm$ 17.5%) than in hLFs (16% $\pm$ 10.3%). Sorted podoplanin-positive hVAFs displayed enhanced tumor formation, lymph node metastasis, and lung metastasis of A549 compared to sorted podoplanin-negative hVAFs. Knockdown of podoplanin in hVAFs decreased the augmenting effect of tumor formation and *in vitro* colony formation. The overexpression of podoplanin in hVAFs hastened the tumor formation of A549, compared with control hVAFs. Furthermore, the analysis of small-sized human lung adenocarcinoma ($n = 112$) revealed that patients with podoplanin-positive cancer-associated fibroblasts had a significantly higher rate of lymph node metastasis and a high risk of recurrence. These results indicate a promotive effect of hVAFs mediated by podoplanin on cancer progression and suggest that the perivascular environment may constitute a specific niche for tumor progression. *Cancer Res; 71(14); 4769–79. ©2011 AACR.*

Introduction

The cancer tissue is composed of different types of stromal cells forming microenvironments (1–3). It has been hypothesized that these stromal components are functionally organized to promote the survival of cancer cells in the host and to generate a favorable microenvironment for cancer cells in both primary and metastatic sites (3–7). The contribution of stromal fibroblasts to the development of a variety of tumors has been supported by extensive clinical evidence and the use of experimental mouse models (8). Accumulating evidence suggests that stromal fibroblasts may promote tumor growth by several mechanisms such as by inducing angiogenesis, recruiting bone marrow–derived endothelial progenitor cells, and remodeling the extracellular matrix (9–11). However, although direct physical interaction between fibroblasts and cancer cells has recently been proposed as a mechanism of cancer cell migration (12), the role of the direct biological interaction between fibroblasts and cancer cells in augmenting tumor progression is not fully understood. It is also increasingly apparent that cancer stromal fibroblasts represent a diverse cell population with different characteristics according to their various origins, such as resident fibroblasts, vascular smooth muscle cells, pericytes (vascular adventitia), and bone marrow–derived cells (13–17).

The vascular adventitia is the outermost connective tissue layer of blood vessels and contains fibroblasts. Animal models have showed that changes in the functions of vascular adventitial fibroblast (VAF) phenotype, such as to a myofibroblast phenotype, contribute to the pathologies of a variety of diseases (18–22). During vascular invasion, cancer cells interact with the VAFs of the existing blood vessels involved with the cancer and migrate into the vascular lumen. Nakayama and colleagues (23) reported that in gastric cancer, blood vessels display structural abnormalities, such as the lack of a vascular adventitia, suggesting that VAFs are absorbed and become part of the stromal fibroblasts. We previously reported the *in vitro* characteristics

Authors' Affiliations: [1]Laboratory of Cancer Biology, Department of Integrated Biosciences, Graduate School of Frontier Sciences, The University of Tokyo; [2]Pathology Division, Research Center for Innovative Oncology, [3]Thoracic Oncology Division, National Cancer Center Hospital East, Chiba, Japan; and [4]Genetic Division, National Cancer Center Research Institute and Central Hospital, Tokyo, Japan

Note: Supplementary data for this article are available at Cancer Research Online (http://cancerres.aacrjournals.org/).

Corresponding Authors: Genichiro Ishii or Atsushi Ochiai, Pathology Division, Research Center for Innovative Oncology, National Cancer Center, Kashiwa, 6-5-1 Kashiwanoha, Kashiwa-City, Chiba 277-8577, Japan. Phone: 81-4-7134-6855; Fax: 81-4-7134-6865; E-mail: gishii@east.ncc.go.jp, aochiai@east.ncc.go.jp

doi: 10.1158/0008-5472.CAN-10-3228

of VAFs as fibroblasts containing mesenchymal progenitor/stem cells (MSC; ref. 24), which are reportedly associated with the progression of metastasis in breast cancer (25). The anatomic location and phenotype of VAFs suggest that VAFs may represent one of the origins of the cancer stromal fibroblasts that create a specific microenvironment conductive for cancer progression.

To investigate whether VAFs constitute a specific microenvironment conducive for cancer progression, to determine which compartment is responsible for progression, and to identify the mechanism of progression, we performed *in vivo* experiments using human VAF (hVAF) and human lung tissue-derived fibroblasts (hLF) in conjunction with the human lung adenocarcinoma cell line A549. We report here that the hVAFs enhanced the tumor formation ability of A549, compared with the hLFs. Moreover, podoplanin was highly expressed in the hVAFs, and podoplanin is the functional protein that is responsible for the enhancement of the tumor formation ability.

Material and Methods

Cell culture

The hVAFs and hLFs were cultured as described before (24). The study was approved by the Institutional Review Board of the National Cancer Center. The human lung adenocarcinoma cell lines A549 and PC-14 were obtained from the RIKEN BioResource Center. A549 was cultured in DMEM (Sigma) and PC-14 was cultured in RPMI 1640 (Invitrogen). CRL-5807 was obtained from the American Type Culture Collection (ATCC) and was cultured in RPMI 1640. All the cell lines were cultured in a medium containing 10% FBS (Sigma), and 1% penicillin and streptomycin (Sigma) and were incubated at 37 in an atmosphere containing 5% CO_2. All the cell lines were used within 2 months after resuscitation of frozen aliquots. Cell lines were authenticated on the basis of viability, growth, and morphology. Passages lower than 10 were used. Primary cells were authenticated using the experiments described before (24) including flow cytometric verification of surface marker expression (CD3, CD14, CD20, CD29, CD34, CD44, CD45, CD68, CD105, CD117, and CD133).

Flow cytometry and cell sorting

The cells were incubated with anti-podoplanin (gp36, clone 18H5, Abcam) antibody and excess antibody was removed by washing with PBS (containing 1% FBS). Polyclonal rabbit anti-mouse immunoglobulins/PE (Dakocytomation) were added as a secondary antibody. The cells were then rinsed with PBS and a FACS scan was performed using FACSCalibur (BD Biosciences). Sorting was performed using FACSAria (BD Biosciences).

Western blot analysis

The cells were lysed in whole-cell extraction buffer (20 mmol/L HEPES-NaOH, 0.5% NP-40, 15% glycerol) containing Complete, a protease inhibitor cocktail tablet (Roche Diagnostics). The proteins were separated on a 12% SDS-polyacrylamide gel and transferred to an Immobilon-P, PVDF membrane (Millipore). The blots were incubated overnight at 4°C with anti-human mouse monoclonal podoplanin antibody (D2-40, Signet) or polyclonal goat actin antibody (Santa Cruz). After washing in TBS-T, the membranes were incubated with HRP-rabbit anti-mouse IgG or HRP-rabbit anti-goat IgG (Zymed). ECL Western Blotting Detection Reagents (GE Healthcare) were used to develop the high-performance chemiluminescence film (GE Healthcare).

Cell growth in soft agar

The anchorage-independent growth of A549 with or without fibroblasts was examined using a colony formation assay in soft agar (Difco Agar Noble). A total of 5×10^3 cells/35 mm dish were suspended in culture medium containing 0.4% agar (1.5 mL) and immediately overlaid onto 0.5% bottom agar in the culture medium (3 mL). The cells were then incubated at 37°C. Two weeks later, colonies with a diameter of >200 μm were counted.

Immunohistochemistry and GFP-positive area analysis

Sections were deparaffinized and heated in citric acid buffer solution at 95°C for 20 minutes. The endogenous peroxidases were quenched with 0.3% H_2O_2 in PBS. The sections were incubated overnight at 4°C using anti-GFP antibody (Invitrogen). The sections were then washed and incubated using the Envision+ system (Dako Cytomation) at room temperature. The color reaction was developed in 2% 3,3′-diaminobenzidine in 50 mmol/L Tris-buffer (pH 7.6) containing 0.3% H_2O_2. The sections were counterstained with Meyer's hematoxylin, dehydrated and mounted. The tumor area and GFP-positive areas of the xenograft sections were analyzed using Axio Vision 4.7.1 software (Zeiss).

Real-time reverse transcriptase-polymerase chain reaction (RT-PCR) and PCR

Cells were washed with PBS and suspended in 1 mL of TRIzol (Invitrogen), then stored at −80. Total RNA was purified from thawed samples using standard techniques, and cDNA was synthesized using the PrimeScript RT reagent Kit (TaKaRa), according to the manufacturer's instructions. RT-PCR was performed in a Smart Cycler System (TaKaTa) using SYBR Premix Ex Taq (TaKaRa) according to the manufacturer's instructions.

Lentiviral vectors

Human WT-podoplanin lentivirus vector was generated by subcloning pcDNA3/human-WT-podoplanin vector (kindly provided by Dr. N. Fujita, Cancer Chemotherapy Center, Japanese Foundation for Cancer Research). The lentiviruses were produced using 293T cells transfected with PCAG-HIV, pCMV-VSV-G-RSV-Rev, and either a podoplanin shRNA vector (CS-H1-shRNA-EG; RIKEN BioResource Center) or a human-WT-podoplanin vector. Transfection was achieved using LipofectAMINE 2000 reagent (Invitrogen) according to the manufacturers' instructions. Vector-containing medium was filtered through a 0.45-μm filter and 8 μg/mL of polybrene (Sigma) was added for target cell transduction.

Statistical analysis

The correlation between podoplanin expression in stromal fibroblasts and the clinicopathologic factors were evaluated using the χ^2 test. Overall survival was measured from the date of surgery until the date of death from any cause or the date the patient was last known to be alive. The survival curves were estimated using the Kaplan–Meier method, and the differences in survival between the 2 groups were compared using the log-rank test. Statistical analysis software (SPSS, version 11.0) was used to perform the analysis.

Animal studies

A549 human lung adenocarcinoma cells alone, or with either hVAFs or hLFs were injected into the s.c. tissue of SCID mice (8–12 weeks of age; CLEA). Tumor volume was calculated as the product of a scaling factor of 0.52 and the tumor length, width, and height. After some procedures such as FACS sorting and transfection with overexpression lentivirus, injection of at least 5×10^4 cells were necessary to have a tumor. For metastatic analysis, at 12 weeks after injection mice were killed and their organs were removed and fixed in 10% formalin. All 5 lobes of lungs were histologically examined for metastasis.

Gene expression analysis using a microarray

We used GeneChip Human Genome U133 Plus 2.0 arrays (Affymetrix), containing 54,675 probe sets, to analyze the mRNA expression levels of approximately 47,000 transcripts and variants from 38,500 well-characterized human genes. Target cRNA was generated from 100 ng of total RNA from each sample using a 3′ IVT Express Kit (Affymetrix). The procedures for target hybridization, washing, and staining with signal amplification were conducted according to the supplier's protocols. The arrays were scanned with a GeneChip Scanner 3000 (Affymetrix), and the intensity of each feature of the array was calculated using GeneChip Operating Software, version 1.1.1 (Affymetrix). The average intensity was standardized to the target intensity, which was set equal to 1,000, to reliably compare various multiple arrays. The values were log transformed and median centered. The programs GeneSpring (Agilent Technologies) and Excel (Microsoft) were used to perform the numerical analysis to permit gene selection. The GEO accession number for microarray data is GSE26146.

Pathologic studies

All the surgical specimens were fixed with 10% formalin or methanol and embedded in paraffin. Serial 4-μm sections were stained with hematoxylin and eosin and the Verhoeff-van-Gieson method to visualize elastic fibers. Lymphatic invasion was evaluated in sections stained with hematoxylin and eosin. Vascular invasion was evaluated using the Verhoeff-van-Gieson method. Podoplanin staining for human surgical specimens were done using anti-human mouse monoclonal podoplanin antibody (D2-40, Signet). According to the definition described in the previous study (26), the positive stained spindle-shaped cells in the cancer stroma were identified as fibroblasts.

Results

hVAFs enhance tumor formation and colony formation

A549 human lung cancer cells (1×10^6) were s.c. injected alone or with either hVAFs or hLFs into SCID mice. At 3 weeks after the injection, tumors had formed in all the mice injected with A549 alone and with either type of fibroblast (Fig. 1A). Notably, although the rate of tumor formation in mice injected with A549 alone or coinjected with A549 and hLFs decreased as the number of injected cells was gradually diluted, the rate of tumor formation remained 100% in mice coinjected with A549 and hVAFs even when the number of injected cells was diluted to 5×10^4 cells. When 1×10^4 cells were injected, no tumors were detected in mice injected with A549 alone or coinjected with A549 and hLFs, but tumors were identified in 25% (2/8) of the mice that were coinjected with A549 and hVAFs (Fig. 1A). By 1×10^4 cells injection, while a tumor was identified at week 4 in 1 of the 8 mice coinjected with A549 and hLFs, most of the mice coinjected with A549 and hVAFs already exhibited tumors (7/8) at this time point (Fig. 1B). However, the growth kinetics of the hVAFs-containing tumors and the hLFs-containing tumors were similar once the tumors were detected (Fig. 1C). Importantly, none of the animals injected with 1×10^4 of A549 cells alone exhibited tumor formation at any time point until week 8 (Fig. 1B).

When tumors coinjected with A549 and GFP-labeled fibroblasts were analyzed, the area of GFP-positive fibroblasts in the tumor tissue at 5 days after injection was similar in the hVAFs and hLFs groups (Fig. 1D). To verify that the capacity of hVAFs to enhance tumor formation is not restricted to the A549 cell line, we performed an *in vivo* tumor formation assay using 2 other human lung adenocarcinoma cell lines, CRL-5807 and PC-14. Three weeks after the coinjection of these cell lines and hVAFs (5×10^4 cells each), both cell lines produced tumors in all 4 cases, whereas the tumor formation rate after coinjection with hLFs was 50% (2/4; Fig. 1E). We next performed *in vitro* A549 colony assay. Colonies with a diameter of 200 μm or larger were counted, and the number of colonies was significantly larger when the cells were seeded with hVAFs (Fig. 1F). In contrast, seeding the A549 cells with hLFs produced only a slight enhancement in colony formation (Fig. 1F).

Podoplanin is overexpressed in hVAFs, and podoplanin-high hVAFs and hLFs enhance A549 tumor formation

We performed a DNA microarray analysis of hVAFs and hLFs (Table 1). Among the genes that were upregulated in hVAFs, we focused on podoplanin, a glycoprotein that is expressed in cancer stromal fibroblasts of human adenocarcinoma in a manner that is correlated with the severity of the disease (26). A flow cytometry analysis revealed that podoplanin was expressed in a higher percentage of hVAFs than hLFs in 10 of the 11 cases (Fig. 2A). The average percentage of podoplanin-high cells in the hVAFs was 43% (SD $\pm$ 17.5) and the average percentage of podoplanin-high cells in the hLFs was 16% (SD $\pm$ 10.3). To determine whether the podoplanin-high cells were responsible for the enhancement of A549

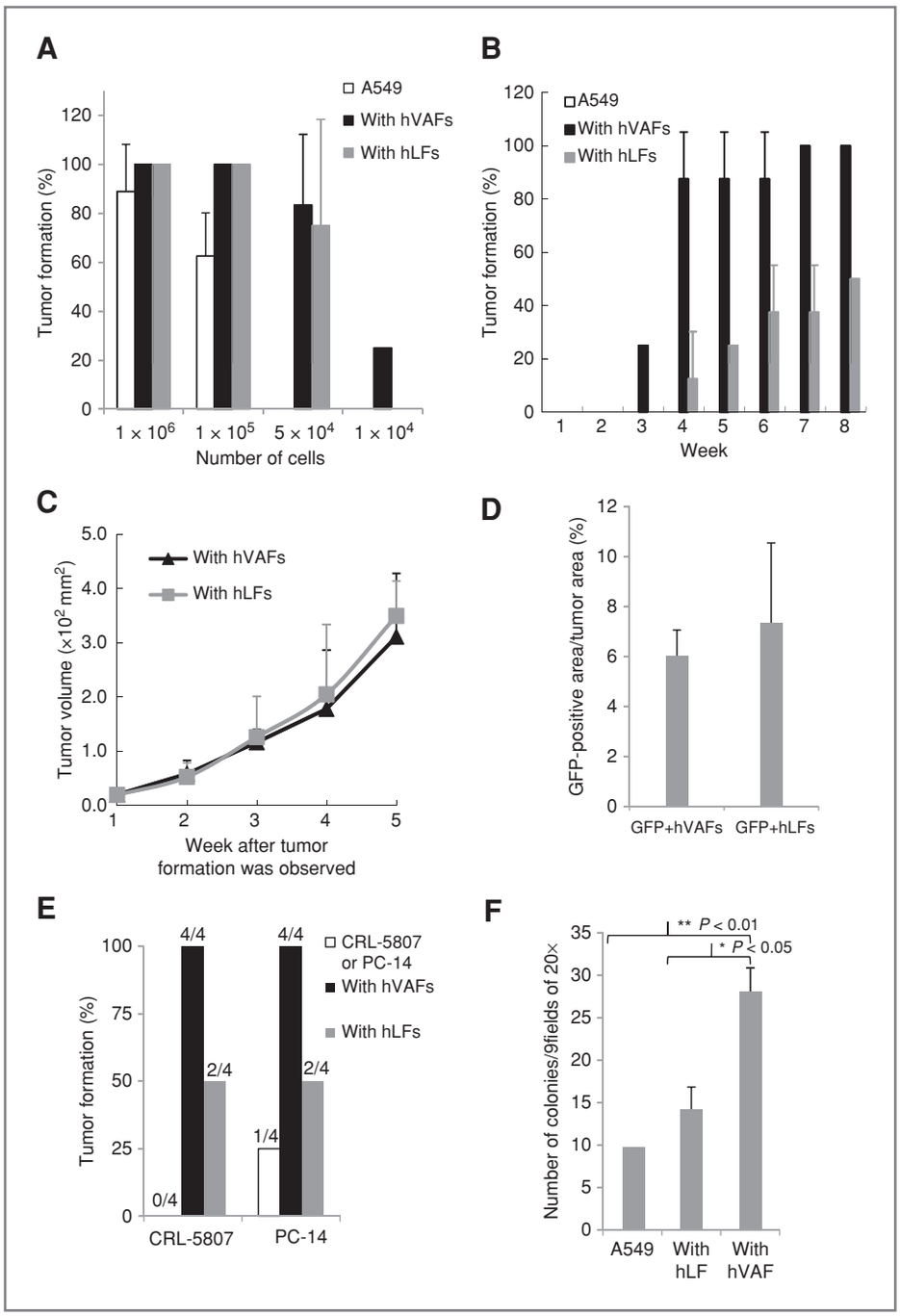

Figure 1. hVAFs promote lung cancer tumor formation. A, tumor formation rates (mean ± SD) at 3 weeks after the s.c. injection of varying numbers of A549 cells alone or with either hVAFs or hLFs into SCID mice ($n = 8$–10). B, tumor formation rates (mean ± SD) after the s.c. injection of 1×10^4 A549 cells with or without either 1×10^4 hVAFs or hLFs into SCID mice ($n = 8$). C, tumor volumes (mean ± SD) after the s.c. injection 1×10^4 A549 cells with either 1×10^4 hVAFs or hLFs into SCID mice. Triangle, A549 plus hVAFs ($n = 8$); square, A549 plus hLFs ($n = 8$). D, GFP-positive area of tumor after the injection of 1×10^6 A549 cells with 1×10^6 GFP-expressing hVAFs or hLFs ($n = 4$). Error bars show the mean ± SD. E, tumor formation rates after the s.c. injection of 5×10^4 CRL-5807 or PC-14 cells with or without either 5×10^4 hVAFs or hLFs into SCID mice ($n = 4$). F, colony formation assay. Colonies with a diameter greater than 200 μm were counted for A549 cells alone or for cells seeded with either hVAFs or hLFs. Error bars show the mean ± SD. The data shown are representative of multiple repeats. Asterisk, $P < 0.05$; double asterisk, $P < 0.01$; both using Student's *t* test.

tumor formation by hVAFs, we coinjected mice with sorted podoplanin-high hVAFs or podoplanin-low hVAFs and A549 s.c. Notably, at week 2, tumors produced by 5×10^4 cells of podoplanin-high hVAFs and A549 were detectable in 70% (7/10) mice, whereas tumors were produced in only 30% (3/10) of the mice coinjected with podoplanin-low hVAFs and A549 (Fig. 2B). We next performed the same assay using hLFs (5×10^4 cells injection). Tumors were detected (at week 2) in 89% (8/9) of the mice coinjected with podoplanin-high hLFs and A549, whereas tumors were detected in only 30% (3/10) of the mice coinjected with podoplanin-low hLFs and A549 (Fig. 2C). The growth kinetics of tumors produced by the coinjection of podoplanin-high or podoplanin-low hVAFs and A549 had comparable slopes (Fig. 2D). We also observed that the numbers of lymph node metastases and lung metastases were much larger in animals coinjected with

Table 1. Oligonucleotide microarray search for genes differently expressed in hVAFs compared to hLFs

Genes upregulated in hVAFs		**Ratio**
Cell adhesion	Coiled-coil domain containing 80	10
	Versican	11
	ABI family, member 3 (NESH) binding protein	6.9
	Fibulin 2	6.8
	Collagen, type 3, α1	6.6
	Laminin, α2	6.5
Transcription	Activating transcription factor 5	6.7
	Early B-cell factor 1	7.5
	Vestigial like 3	5.3
Metabolic process	STEAP family member 4	9.5
	Acyl-CoA synthetase long-chain family member 1	5.4
	Glutaminase	5.1
	Ectonucleotide pyrophosphatase/phosphodiesterase 2	4.7
	REV3-like, catalytic subunit of DNA polymerase χ	6.1
Development	Matrix Gla protein	24
	Dickkopf homolog 1	11
	Serpin peptidase inhibitor, clade E, member 2	7.4
	Chordin-like 1	5.4
	Doublecortin-like kinase 1	5.2
	Fibroblast growth factor 7 (kerathocyte growth factor)	4.9
	Phosphatidic acid phosphatase type 2B	4.7
	Podoplanin	4.7
Immune response	Complement component 7	10
Other	Tissue factor pathway inhibitor 2	5.7
	Ubiquitin-specific peptidase 53	6.6
	EGF-containing fibulin-like extracellular matrix protein 1	5.4
	SH3-domain binding protein 5 (BTK-associated)	5.3
Genes downregulated in hVAFs		
Cell adhesion	Tenascin C	0.25
	CD9 molecule	0.24
Apoptosis	Pleckstrin homology-like domain, family A, member 1	0.47
	Pleckstrin homology-like domain, family A, member 2	0.24
	Tumor necrosis factor receptor superfamily, member 19	0.16
	Ras homolog gene famliy, member B	0.17
	Caspase recruitment domain family, member 16	0.29
Transcription	Forkhead box F1	0.15
	Forkhead box F2	0.11
	Tribbles homolog 3	0.21
	Lipopolysaccharide-induced TNF factor	0.31
	TOX high mobility group box family member 2	0.23
	cAMP responsive element binding protein 3	0.26
Metabolic process	Flavin containing m onooxygenase 3	0.26
	Prostaglandin D 2 synthase 21 kDa (brain)	0.24
Development	TMP metalopeptidase inhibitor 3	0.24
	TMP metalopeptidase inhibitor 4	0.21
	Tensin 3	0.15
	Dickkopf homolog 3	0.22
Signal transduction	Growth differentiation factor 15	0.22
	Prostaglandin E receptor 2 (subtype EP2)	0.20
Other	α2-macrogrobulin	0.08
	Myosin light chain kinase	0.11
	microtubule-associated protein 4	0.25

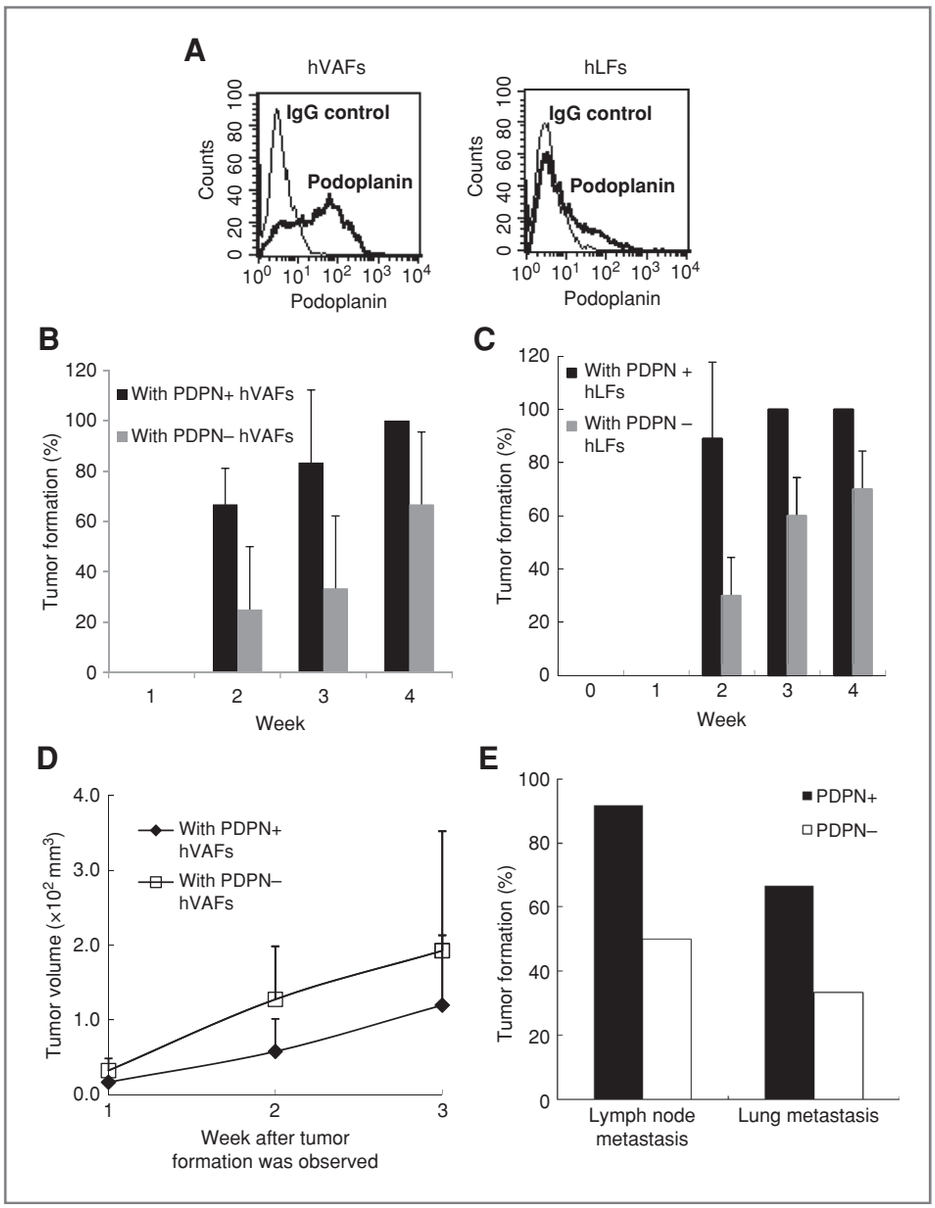

Figure 2. Podoplanin-high fibroblasts enhance the tumor formation of A549 cells. A, flow cytometric analysis for podoplanin expression in hVAFs and hLFs. Thin line, IgG control; bold line, podoplanin antibody. B, tumor formation rates after the s.c. injection of 5×10^4 A549 cells with FACS-sorted podoplanin-high (PDPN+) hVAFs or podoplanin-low (PDPN-) hVAFs into SCID mice ($n = 10$). C, tumor formation rates after the s.c. injection of 5×10^4 A549 cells with FACS-sorted podoplanin-high (PDPN+) hLFs or podoplanin-low (PDPN−) hLFs into SCID mice ($n = 9$–10). D, tumor volumes (mean ± SD) after the s.c. injection of 5×10^4 A549 cells with FACS-sorted podoplanin-high (PDPN+) hVAFs or podoplanin-low (PDPN−) hVAFs. Square, A549 plus PDPN− hVAFs ($n = 10$); diamond, A549 plus PDPN+ hVAFs ($n = 10$). E, rates of lymph node and lung metastasis in SCID mice with s.c. tumors 2 months after the injection of 5×10^4 A549 cells and 5×10^4 PDPN+ hVAFs and hLFs or PDPN− hVAFs and hLFs.

podoplanin-high hVAFs or podoplanin-high hLFs (Fig. 2E). Among the mice coinjected with podoplanin-high fibroblasts, 92% (11/12) had lymph node metastases; meanwhile 50% (6/12) of the mice coinjected with podoplanin-low fibroblasts exhibited lymph node metastases. In addition, lung metastases were seen in 67% (4/6) of the mice coinjected with podoplanin-high fibroblasts and 33% (2/6) of the mice coinjected with podoplanin-low fibroblasts (Fig. 2E). Bone metastases were not visible in histopathologic investigation.

Podoplanin as a functional protein for A549 tumor formation

Short hairpin (sh) RNA for podoplanin or luciferase were transduced into hVAFs for the stable reduction of podoplanin expression by >80% or as a control, respectively. The expression level of podoplanin in the transduced cells was confirmed using a Western blot analysis and RT-PCR (Fig. 3A and B). Knockdown of podoplanin did not have an effect on hVAFs cell growth on day 3 (data not shown). An *in vitro* colony assay revealed a 4-fold difference in colony formation between A549 cells seeded with luciferase-shRNA hVAFs and those seeded with podoplanin-shRNA hVAFs (Fig. 3C). Podoplanin-shRNA hVAFs or luciferase-shRNA hVAFs and A549 were then co-injected into mice s.c. (1×10^4 cells each). Fewer tumors were detected in mice co-injected with podoplanin-shRNA hVAFs than in mice co-injected with control hVAFs at all-time points (Fig. 3D). Similar results were seen using another podoplanin-shRNA

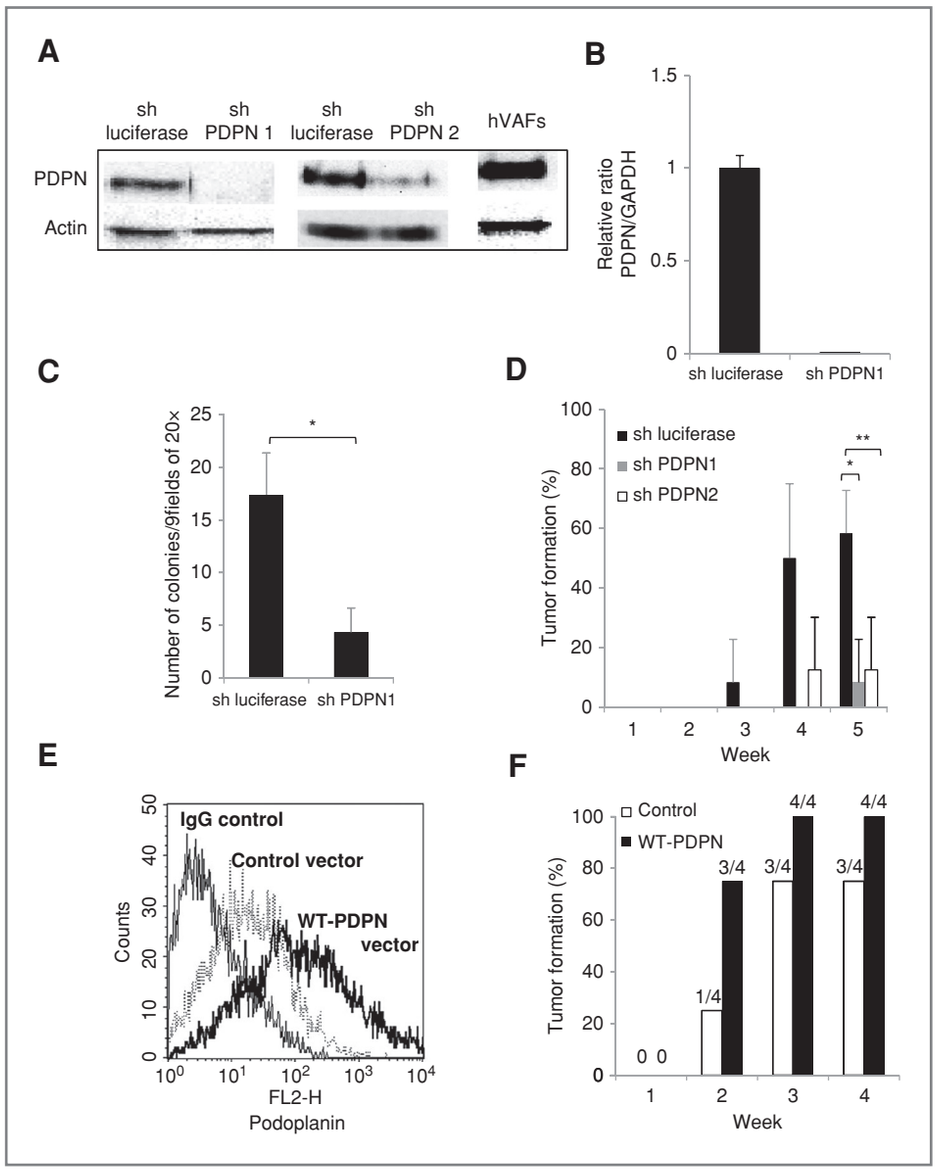

Figure 3. Podoplanin is a functional protein in the fibroblast-induced augmentation of tumor formation. A, Western blot analysis showing PDPN expression in control or podoplanin shRNA-infected hVAFs. B, mRNA levels of podoplanin in control or podoplanin shRNA-infected hVAFs. C, colony formation assay. Colonies with a diameter greater than 200 μm were counted for A549 cells with either control or podoplanin shRNA-infected hVAFs. Error bars show the mean ± SD. Data shown are representative of multiple repeats. Asterisk, $P < 0.01$ using the Student's t test. D, tumor formation rate measurement after the s.c. injection of 1×10^4 A549 cells with control or podoplanin shRNA-infected hVAFs into SCID mice ($n = 8$–10). Asterisk, $P < 0.01$; double asterisk, $P < 0.01$ using the Student's t test. E, flow cytometric analysis of control or wild-type podoplanin (WT-PDPN)–infected hVAFs. Thin line, IgG control; dotted line, control hVAFs; bold line, WT-PDPN overexpressed hVAFs. F, tumor formation rates after the s.c. injection of 5×10^4 A549 cells with control or WT-PDPN overexpressed hVAFs into SCID mice ($n = 4$).

(Fig. 3D). We further examined the dependence of tumor formation on podoplanin using the enforced expression of podoplanin in hVAFs (Fig. 3E). Podoplanin-overexpressed hVAFs with A549 cells (5×10^4 cells injection each) resulted in a tumor formation rate of 75% at week 2 (3/4), whereas tumor formation was only observed in 25% (1/4) of the animals coinjected with control hVAFs (Fig. 3F).

Podoplanin-positive stromal fibroblasts in human lung adenocarcinoma

We examined the presence of podoplanin positive cancer-associated fibroblasts (CAF) in human lung adenocarcinomas with a tumor size of 3 cm or less (Fig. 4F). Of the 112 specimens, 32 were positive for podoplanin immunostaining. Podoplanin-positive CAF cases displayed significantly more vascular invasion ($P < 0.0001$) and lymph node metastasis ($P < 0.005$; Fig. 4B). Furthermore, a Kaplan–Meier analysis showed a significant difference in both the disease-free interval ($P < 0.001$) and the overall survival ($P < 0.001$) between 2 groups (Fig. 4C and D).

Discussion

In this study, we present for the first time the finding that fibroblasts with 2 different origins but from the same organ specimen had distinct effects on the enhancement of tumor formation. We used 2 human-derived primary fibroblasts, hVAFs and hLFs. Both fibroblast types enhanced the tumor formation abilities of A549, CRL-5807 and PC-14, but this ability was especially augmented by hVAFs. Of the genes

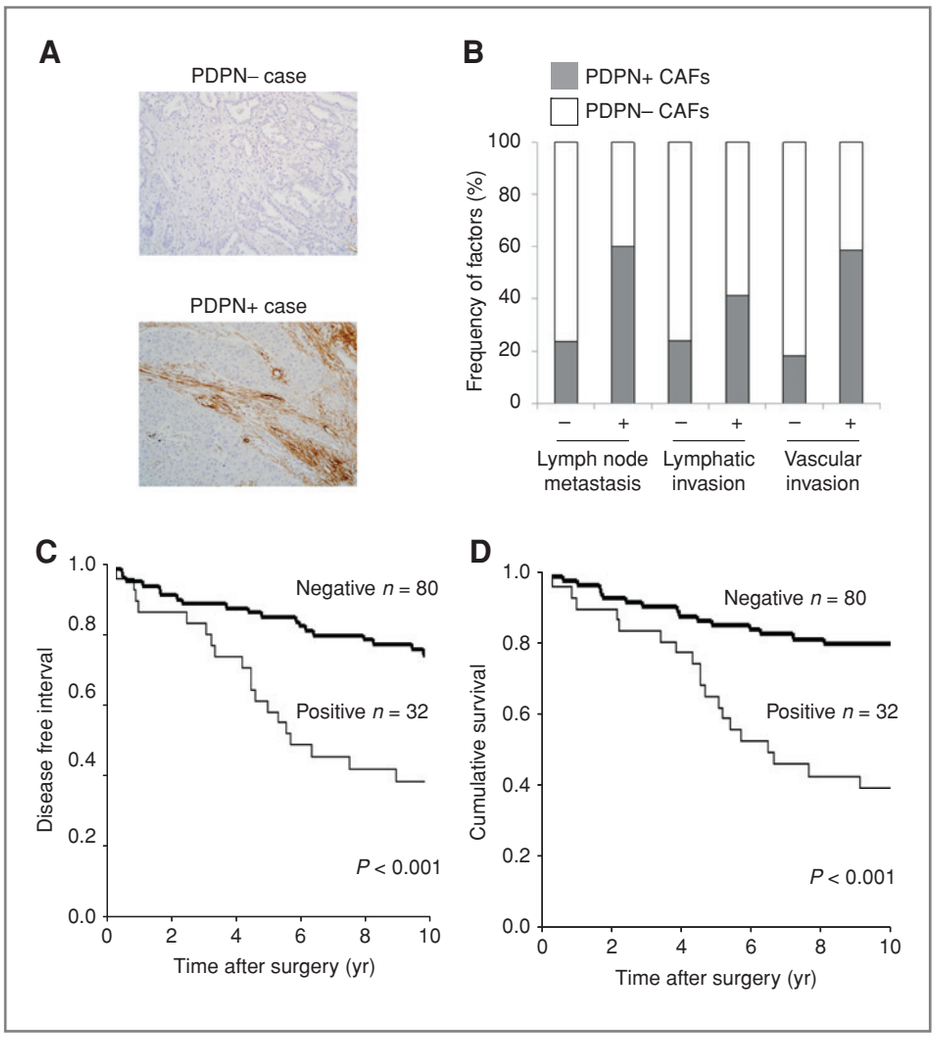

Figure 4. Podoplanin-positive stromal fibroblasts in human adenocarcinoma as a prognostic factor. A, immunostaining of podoplanin in stromal fibroblasts of human lung adenocarcinoma patients with tumor size of 3 cm or less. B, number of patients and rates of clinicopathologic factors in relation to podoplanin expression in the stromal fibroblasts evaluated using the χ^2 test. Percentage shows rates of each factor within podoplanin expression. D, disease-free interval curve (C) and overall survival curve (D) of podoplanin expression in stromal fibroblasts of human lung adenocarcinoma patients with a tumor size of 3 cm or less.

differentially expressed in hVAFs compared to hLFs in our microarray analysis, we focused on podoplanin because a previous study proposed that the expression of podoplanin in stromal fibroblasts in adenocarcinoma patients was correlated with a poor prognosis and a high rate of recurrence at all stages (26). Podoplanin is known as a lymphatic endothelial marker. It is a mucin-type sialoglycoprotein reported to be expressed in several cancer cells (27–30) and that binds to CLEC-2 on platelets to form platelet-aggregations, enhancing metastasis (31). After sorting podoplanin-high cells from both hVAFs and hLFs, we found that regardless of the fibroblast origin, podoplanin-high fibroblasts were capable of enhancing the tumor formation rate, compared with podoplanin-low cells (Fig. 2B and C). This finding suggests that differences in podoplanin expression could be responsible for the superiority of hVAFs in promoting tumor formation, compared with hLFs.

To determine whether podoplanin-low fibroblasts can become podoplanin-high fibroblasts, we tested the effect of A549 conditioned media on hVAFs *in vitro*. We observed that less than 10% of podoplanin-low fibroblasts exposed to A549 conditioned media upregulated podoplanin expression by flow cytometry analysis (data not shown). We next investigated whether coinjection of either hVAFs or hLFs (1×10^5 cells) with A549 could lead to an increase in the frequency of podoplanin-expressing cells within the tumor *in vivo*, 1-week postinjection. However, both hVAFs and hLFs localized mainly in the necrotic area of the tumor, thus hindering accurate quantification and comparison of the percentage of podoplanin-expressing cells in this experiment. Furthermore, there was no correlation between these observations and the frequency of podoplanin-high cells in the injected hVAF or hLF populations (data not shown).

The shRNA knockdown of podoplanin expression not only supported the data that podoplanin-high fibroblasts enhance the tumor formation ability, it also revealed that podoplanin is a functional protein in tumor formation enhancement. This conclusion was also supported by the results of an *in vitro* colony assay. Tumor progression is thought to occur in several steps, such as colonization, proliferation, inflammation and

angiogenesis, infiltration, and metastasis to the new environment (32, 33). Based on the *in vivo* survival rate of GFP-positive hVAFs and hLFs in the s.c. tumors and the *in vivo* tumor volume growth rate after tumor formation, podoplanin-high fibroblasts are predicted to function during the early phase of tumorigenesis. Furthermore, the *in vitro* colony assay suggested that podoplanin in fibroblasts promotes an environment conducive to cancer cell anchorage independence, where neither angiogenesis nor inflammation occurs. Taken together, these phenomena suggest that podoplanin in fibroblasts functions as a tumor formation enhancer during the initiation of tumorigenesis, such as during the pre-angiogenic phase.

How podoplanin-high fibroblasts interact with cancer cells to promote tumor progression remains unclear. One possibility is direct extracellular binding of fibroblasts to cancer cells, promoting cancer progression. *In vitro* coculturing of A549 and hVAFs showed no difference in A549 cell number even in direct contact with hVAFs (Supplementary Fig. 1A). Furthermore, seeding A549-GFP on either hVAFs or hLFs did not lead to differences in tumor cell proliferation (Supplementary Fig. 1B). These *in vitro* experiments suggest that direct contact between fibroblasts and lung cancer cells is not sufficient to influence cancer cell proliferation and/or apoptosis. Moreover, the human cancer cell lines used in this study were negative for CLEC-2 or podoplanin expression when examined using quantitative RT-PCR (data not shown), suggesting that the podoplanin-expressing fibroblasts did not bind directly to cancer cells, at least not through CLEC-2, the only receptor for podoplanin described so far. Still, the podoplanin produced in fibroblasts may bind to cancer cells via process mediated by some other proteins. Extracellular binding proteins that interact with podoplanin should be further analyzed to determine the possibility of a direct interaction with cancer cells. Another possibility is stimulation of a signaling pathway within podoplanin-high fibroblasts leading or mediating tumor development. However, although the addition of Luciferase-shRNA hVAFs or podoplanin-shRNA hVAFs to soft agar containing A549 cells revealed the significant ability of podoplanin-expressing hVAFs to enhance colony formation (Fig. 3C), the addition of their culture media did not enhance tumor formation (Supplementary Fig. 2A). Furthermore, the addition of recombinant podoplanin into soft agar did not influence the colony formation rate of A549 (Supplementary Fig. 2B), suggesting that an interaction between podoplanin-high fibroblasts and cancer cells is responsible for enhancing the tumor formation ability. In addition, the fibroblasts alone did not form colonies in either the *in vivo* or *in vitro* assays, supporting the concept that the fibroblasts provide a favorable environment in which cancer cells may form colonies but that the fibroblasts themselves do not form or produce proliferative colonies. So far, the ERM protein family is known to bind to the intracellular domain of podoplanin to stimulate the RhoA activity of the cells, inducing cell migration (34). Given that podoplanin expression in fibroblasts contributes to tumorigenesis, coordination of this signaling response involving cell motility and/or direct crosstalk through an extracellular domain might act as molecular cues that trigger tumor progression and promote a poor clinical outcome. Thus, further analysis is needed to determine how podoplanin-high fibroblasts enhance tumor formation progression.

It is interesting that podoplanin-high cells are more common among hVAFs than among hLFs. This may indicate that during vascular invasion, the metastatic ability of cancer cells may be enhanced by interaction with VAFs. Alternatively, circulating cancer cells that encounter podoplanin-low fibroblasts and/or podoplanin-high inducible fibroblasts may have a better chance of colonizing the new environment. Our *in vivo* mouse model also revealed a difference in the rates of metastasis to the lymph nodes and lungs (Fig. 2C). Consistent with this data, the results of our clinical evaluation of adenocarcinomas with a size of 3 cm or smaller further showed the relevance of podoplanin as a prognostic factor. Although the tumor size at the time of resection was limited to 3 cm or less, the rates of vascular invasion and lymph node metastasis were significantly higher among the patients with podoplanin-positive stromal fibroblasts (Fig. 4B). Moreover, the disease-free interval was significantly lower among patients with podoplanin-positive fibroblasts (Fig. 4C). The current clinicpathological data also suggest that podoplanin-positive fibroblasts enhance tumor progression.

In colorectal cancer, the presence of podoplanin-positive stromal fibroblasts is associated with a better prognosis, compared with the presence of podoplanin-negative stromal fibroblasts (35). We suspect that this difference can be explained by a difference in how cancer cells react to podoplanin-expressing fibroblasts and/or a difference in the function of podoplanin-expressing fibroblasts in different organs. Therefore, further studies should focus on evaluating in which types of cancer podoplanin-positive fibroblasts contribute to tumor progression and what are the mechanisms that mediate this contribution. Elucidating how different cancer cell types elicit distinct responses from the same fibroblasts may further reveal the function of podoplanin in organ-specific fibroblasts.

Previously, we reported that hVAFs, but not hLFs, contain MSCs (24). It has been reported that bone marrow–derived MSCs can promote breast cancer metastasis *in vivo* (25). To elucidate whether the MSCs within the hVAFs are responsible for the enhancement of A549 tumor formation, we induced their differentiation into either the adipogenic or an osteogenic lineage. We found that culturing hVAFs with induction medium did not change the ability of hVAFs to enhance tumor formation in the A549 cell line (Supplementary Fig. 3A–D). Because the identification of MSCs in hVAFs has not been clarified, we cannot exclude MSCs as the population responsible for tumor formation. However, we have shown that neither osteogenic nor adipogenic differentiation of hVAFs does not change the potential of hVAFs to augment the tumor formation ability of A549 cells.

In conclusion, we have identified that hVAFs enhance the tumor formation of lung adenocarcinoma cells, compared with hLFs, and that this activity was at least partly dependent on podoplanin, a functional protein expressed on fibroblasts. Podoplanin-positive cancer cells are known to metastasize through the formation of podoplanin–platelet complex. Therefore, the promotive effect of podoplanin-positive stromal fibroblasts on cancer progression suggests

that not only tumor cells, but also the fibroblasts that provide a supportive microenvironment (e.g., perivascular stroma cells) can be targeted by cancer therapy. Moreover, further evaluation of the roles that this protein plays in cancer development may reveal the mechanism of cancer–fibroblast interactions and how the microenvironment supports tumor progression.

Disclosure of Potential Conflicts of Interest

No potential conflicts of interest were disclosed.

Acknowledgments

We thank Dr. Naoya Fujita (The Cancer Chemotherapy Center of Japanese Foundation for Cancer Research) for kindly providing pcDNA3/human-WT-podoplanin vector and Hiroko Hashimoto for technical support.

Grant Support

This work was supported by the Grant-in-Aid for Cancer Research (19-10) from the Ministry of Health, Labor, and Welfare Programs; the Foundation for the Promotion of Cancer Research, 3rd-Term Comprehensive 10-Year Strategy for Cancer Control; Program for Promotion of Fundamental Studies in Health Sciences of the National Institute of Biomedical Innovation; and JSPS KAKENHI (20590417, 215981). A. Hoshino was supported by Research Fellowships of the Japan Society for the Promotion of Science for Young Scientists.

The costs of publication of this article were defrayed in part by the payment of page charges. This article must therefore be hereby marked *advertisement* in accordance with 18 U.S.C. Section 1734 solely to indicate this fact.

Received September 1, 2010; revised April 27, 2011; accepted May 12, 2011; published OnlineFirst May 24, 2011.

References

1. Kalluri R, Zeisberg M. Fibroblasts in cancer. Nat Rev Cancer 2006;6:392–401.
2. Bissell MJ, Radisky D. Putting tumours in context. Nat Rev Cancer 2001;1:46–54.
3. Tlsty TD, Coussens LM. Tumor stroma and regulation of cancer development. Annu Rev Pathol 2006;1:119–50.
4. Patocs A, Zhang L, Xu Y, Weber F, Caldes T, Mutter GL, et al. Breast-cancer stromal cells with TP53 mutations and nodal metastases. N Engl J Med 2007;357:2543–51.
5. Morrissey C, Vessella RL. The role of tumor microenvironment in prostate cancer bone metastasis. J Cell Biochem 2007;101:873–86.
6. Hanahan D, Weinberg RA. The hallmarks of cancer. Cell 2000;100:57–70.
7. Mantovani A, Allavena P, Sica A, Balkwill F. Cancer-related inflammation. Nature 2008;454:436–44.
8. Desmouliere A, Guyot C, Gabbiani G. The stroma reaction myofibroblast: a key player in the control of tumor cell behavior. Int J Dev Biol 2004;48:509–17.
9. Orimo A, Gupta PB, Sgroi DC, Arenzana-Seisdedos F, Delaunay T, Naeem R, et al. Stromal fibroblasts present in invasive human breast carcinomas promote tumor growth and angiogenesis through elevated SDF-1/CXCL12 secretion. Cell 2005;121:335–48.
10. Pietras K, Pahler J, Bergers G, Hanahan D. Functions of paracrine PDGF signaling in the proangiogenic tumor stroma revealed by pharmacological targeting. PLoS Med 2008;5:e19.
11. Allinen M, Beroukhim R, Cai L, Brennan C, Lahti-Domenici J, Huang H, et al. Molecular characterization of the tumor microenvironment in breast cancer. Cancer Cell 2004;6:17–32.
12. Gaggioli C, Hooper S, Hidalgo-Carcedo C, Grosse R, Marshall JF, Harrington K, et al. Fibroblast-led collective invasion of carcinoma cells with differing roles for RhoGTPases in leading and following cells. Nat Cell Biol 2007;9:1392–400.
13. Bauer M, Su G, Casper C, He R, Rehrauer W, Friedl A. Heterogeneity of gene expression in stromal fibroblasts of human breast carcinomas and normal breast. Oncogene 2010;29:1732–40.
14. Ronnov-Jessen L, Petersen OW, Koteliansky VE, Bissell MJ. The origin of the myofibroblasts in breast cancer. Recapitulation of tumor environment in culture unravels diversity and implicates converted fibroblasts and recruited smooth muscle cells. J Clin Invest 1995;95:859–73.
15. Ishii G, Sangai T, Sugiyama K, Ito T, Hasebe T, Endoh Y, et al. In vivo characterization of bone marrow-derived fibroblasts recruited into fibrotic lesions. Stem Cells 2005;23:699–706.
16. Ishii G, Sangai T, Oda T, Aoyagi Y, Hasebe T, Kanomata N, et al. Bone-marrow-derived myofibroblasts contribute to the cancer-induced stromal reaction. Biochem Biophys Res Commun 2003;309:232–40.
17. Sangai T, Ishii G, Kodama K, Miyamoto S, Aoyagi Y, Ito T, et al. Effect of differences in cancer cells and tumor growth sites on recruiting bone marrow-derived endothelial cells and myofibroblasts in cancer-induced stroma. Int J Cancer 2005;115:885–92.
18. Mallawaarachchi CM, Weissberg PL, Siow RC. Antagonism of platelet-derived growth factor by perivascular gene transfer attenuates adventitial cell migration after vascular injury: new tricks for old dogs? FASEB J 2006;20:1686–8.
19. Wilcox JN, Waksman R, King SB, Scott NA. The role of the adventitia in the arterial response to angioplasty: the effect of intravascular radiation. Int J Radiat Oncol Biol Phys 1996;36:789–96.
20. Xu F, Ji J, Li L, Chen R, Hu W. Activation of adventitial fibroblasts contributes to the early development of atherosclerosis: a novel hypothesis that complements the "Response-to-Injury Hypothesis" and the "Inflammation Hypothesis." Med Hypotheses 2007;69:908–12.
21. Hu Y, Zhang Z, Torsney E, Afzal AR, Davison F, Metzler B, et al. Abundant progenitor cells in the adventitia contribute to atherosclerosis of vein grafts in ApoE-deficient mice. J Clin Invest 2004;113:1258–65.
22. Stenmark KR, Gerasimovskaya E, Nemenoff RA, Das M. Hypoxic activation of adventitial fibroblasts: role in vascular remodeling. Chest 2002;122:326S–34S.
23. Nakayama H, Enzan H, Miyazaki E, Kuroda N, Toi M, Hiroi M, et al. Presence of vascular adventitial fibroblastic cells in diffuse-type gastric carcinomas. J Clin Pathol 2004;57:970–2.
24. Hoshino A, Chiba H, Nagai K, Ishii G, Ochiai A. Human vascular adventitial fibroblasts contain mesenchymal stem/progenitor cells. Biochem Biophys Res Commun 2008;368:305–10.
25. Karnoub AE, Dash AB, Vo AP, Sullivan A, Brooks MW, Bell GW, et al. Mesenchymal stem cells within tumour stroma promote breast cancer metastasis. Nature 2007;449:557–63.
26. Kawase A, Ishii G, Nagai K, Ito T, Nagano T, Murata Y, et al. Podoplanin expression by cancer associated fibroblasts predicts poor prognosis of lung adenocarcinoma. Int J Cancer 2008;123:1053–9.
27. Shimada Y, Ishii G, Nagai K, Atsumi N, Fujii S, Yamada A, et al. Expression of podoplanin, CD44, and p63 in squamous cell carcinoma of the lung. Cancer Sci 2009;100:2054–9.
28. Atsumi N, Ishii G, Kojima M, Sanada M, Fujii S, Ochiai A. Podoplanin, a novel marker of tumor-initiating cells in human squamous cell carcinoma A431. Biochem Biophys Res Commun 2008;373:36–41.
29. Schacht V, Dadras SS, Johnson LA, Jackson DG, Hong YK, Detmar M. Up-regulation of the lymphatic marker podoplanin, a mucin-type transmembrane glycoprotein, in human squamous cell carcinomas and germ cell tumors. Am J Pathol 2005;166:913–21.
30. Wicki A, Lehembre F, Wick N, Hantusch B, Kerjaschki D, Christofori G. Tumor invasion in the absence of epithelial-mesenchymal transition: podoplanin-mediated remodeling of the actin cytoskeleton. Cancer Cell 2006;9:261–72.

31. Kunita A, Kashima TG, Morishita Y, Fukayama M, Kato Y, Tsuruo T, et al. The platelet aggregation-inducing factor aggrus/podoplanin promotes pulmonary metastasis. Am J Pathol 2007;170:1337–47.

32. Nguyen DX, Bos PD, Massague J. Metastasis: from dissemination to organ-specific colonization. Nat Rev Cancer 2009;9:274–84.

33. Kim MY, Oskarsson T, Acharyya S, Nguyen DX, Zhang XH, Norton L, et al. Tumor self-seeding by circulating cancer cells. Cell 2009;139:1315–26.

34. Martin-Villar E, Megias D, Castel S, Yurrita MM, Vilaro S, Quintanilla M. Podoplanin binds ERM proteins to activate RhoA and promote epithelial-mesenchymal transition. J Cell Sci 2006;119:4541–53.

35. Yamanashi T, Nakanishi Y, Fujii G, Akishima-Fukasawa Y, Moriya Y, Kanai Y, et al. Podoplanin expression identified in stromal fibroblasts as a favorable prognostic marker in patients with colorectal carcinoma. Oncology 2009;77:53–62.